Spontaneous Symmetry Breaking of Population between Two Dynamic Attractors in a Driven Atomic Trap: Ising-class Phase Transition

Kihwan Kim[1,2], Myoung-Sun Heo[1,2], Ki-Hwan Lee[1,2], Kiyoub Jang[1,2], Heung-Ryoul Noh[†], Doochul Kim[1], and Wonho Jhe[1,2]
[1]School of Physics and [2]Center for Near-field Atom-photon Technology, Seoul National University, Seoul 151-747, Korea
[†]Department of Physics, Chonnam National University, Gwangju 500-757, Korea

(Dated: December 28, 2021)

We have observed spontaneous symmetry breaking of atomic populations in the dynamic phase-space double-potential system, which is produced in the parametrically driven magneto-optical trap of atoms. We find that the system exhibits similar characteristics of the Ising-class phase transition and the critical value of the control parameter, which is the total atomic number, can be calculated. In particular, the collective effect of the laser shadow becomes dominant at large atomic number, which is responsible for the population asymmetry of the dynamic two-state system. This study may be useful for investigation of dynamic phase transition and temporal behaviour of critical phenomena.

PACS numbers: 05.70.Fh, 05.45.-a, 68.35.Rh, 32.80.Pj

The phenomena of symmetry breaking, widespread in nature with examples from cosmology to biology, have been much studied [1, 2, 3]. Recently in a vibro-fluidized granular gas, spontaneous symmetry breaking (SSB) of temperature and population between two compartments connected by a hole was reported and understood in terms of the density-dependent inelastic collision rates [4, 5]. Moreover there have been many works on fluctuation-induced transitions in equilibrium [6, 7, 8] as well as far from equilibrium [9, 10, 11]. The double well structure of these systems is very similar to the two compartments of the granular box, where SSB was observed. In particular, we have recently studied the atomic population transition between two dynamic phase-space attractors available in the parametrically driven magneto-optical trap (MOT) system [11].

In this Letter, we report on experimental as well as theoretical investigation of SSB of the atomic population between two dynamic states of the driven MOT. We have found that the control parameter for SSB is the total number of atoms in both states: The population equality between the two equivalent states is broken spontaneously above a critical number of atoms. This phenomenon can be well understood as the Ising-class phase transition. We have measured the critical number under various experimental parameters and also observed the temporal evolution from symmetric to asymmetric states above threshold. The SSB mechanism is described qualitatively by considering two collective interactions occurring at large atomic number, the shadow effect and the reradiation effect [12, 13, 14, 15]. In particular, the measured critical numbers are in good agreement with the analytical and the simulational results.

The experimental scheme is similar to those reported in previous works on parametrically modulated MOT [11, 16], where we observed parametric excitation, limit cycles (dynamic phase-space attractors), super-critical and sub-critical bifurcation. In particular, the bifurcations were explained by atomic double- and triple-well potentials in the rotating phase space. Due to fluctuating atomic motions resulting from spontaneous emissions, population transfer occurs between the two states of dynamic double well, which tends to equalize the population of each state [Fig. 1(a)]. This atomic transition between the two states oscillating in position space (Fig. 1) was confirmed by observing the temporal recovery of the population symmetry after emptying one state. In this case, the recovering rates are equivalent to the transition rates [11].

It is interesting to observe that the population symmetry, which is equivalent to zero spontaneous magnetization in the Ising spin system, is only maintained below a certain critical value of the total atomic number. Above the critical number, however, we have observed SSB of atomic population, as shown in Fig. 1(b). The SSB can be observed under wide experimental conditions of modulation frequency f and amplitude h, from super-critical to sub-critical bifurcation regions. The atomic populations were simultaneously measured by resonant absorption of a weak probe laser. The typical experimental parameters are as follows: magnetic-field gradient along the atomic oscillation direction (z-direction) $b = 14$ G/cm, cooling laser detuning $\delta = -2.6\Gamma$, and laser intensity in the z-axis $I_z = 0.039 I_s$ (I_s is the averaged saturation intensity, 3.78 mW/cm^2). The intensity on the transverse axes is typically 5 times larger than that of the z-axis. The measured trap frequency is 43.6 ($\pm$ 2.4) Hz whereas the damping coefficient is 160.4 ($\pm$ 33) s^{-1}, which is about three times larger than that expected in the Doppler theory [17].

Figure 2(a) presents the normalized population difference between the two dynamic states (1 and 2 with $N_1 > N_2$), $\eta_p = (N_1 - N_2)/N_T$ versus the total atomic number, $N_T = N_1 + N_2$. As shown in the figure, the main control parameter of SSB is N_T so that SSB (or

Corresponding author: whjhe@snu.ac.kr

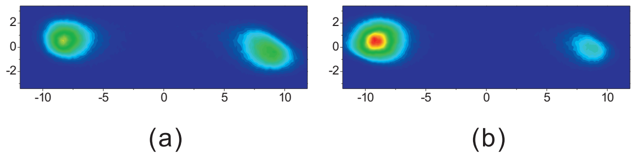

FIG. 1: Snapshot images of atoms in two dynamic attractors (a) before SSB of atomic population and (b) after SSB, taken by a charge-coupled-device (CCD). The total number of atoms is (a) 6.1×10^7 and (b) 6.9×10^7, respectively. The relative population difference in (b) is 0.63. Here $f = 96$ Hz, $h = 0.9$, and the abscissas are in unit of mm.

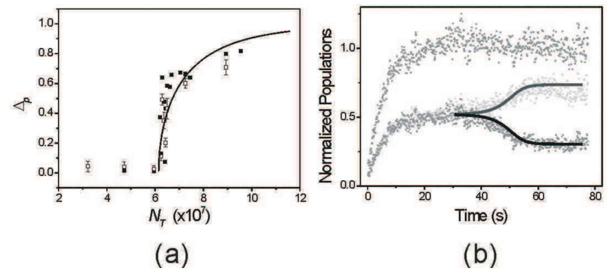

FIG. 2: (a) Experimental data of the normalized population difference Δ_p versus the total atomic number N_T. Here $f = 88$ Hz ($\simeq 2.0 f_0$) and $h = 0.86$. The solid curve is the fitting by the Ising model function with $N_c = 6.1 (\pm 0.4) \times 10^7$. (b) Temporal evolution of SSB. The split theoretical curves represent the normalized populations of the two dynamic states ($N_T = 6.5 \times 10^7$ and $\Delta_p = 0.52$). The simple sum of each population, i.e., the normalized total atomic number, is also shown on the top.

the Ising-class phase transition) occurs above the critical number N_c. We have measured N_1 and N_2 by two independent methods: CCD images (filled black boxes) and probe absorption (empty boxes). N_T was varied by adjusting the intensity of the repumping laser while all the other trap parameters remain fixed. Note that we did not find any other control parameters other than N_T: for instance, the intensity imbalance between the $+z$ and $-z$ laser beams did not contribute to SSB for the imbalance of up to 20%, beyond which the atomic limit cycle motions were not sustained.

We have measured the critical number N_c at various experimental parameters of f and h. For example, at $h = 0.86$, N_c decreases gently from 7.9×10^7 to 4.1×10^7 as f increases from $1.95 f_0$ to $2.4 f_0$ (f_0 is the MOT trap frequency along the z-axis). At $f = 2.1 f_0$ ($\simeq 90$ Hz), N_c also decreases from 11.9×10^7 to 6.2×10^7 as h increases from 0.64 to 0.86. In brief, N_c increases with the transition rate W: when f or h increases, W decreases (see Ref. [11] for details), and consequently N_c becomes decreased. However, SSB is not observed outside the above region of parameters, that is, near the super-critical or sub-critical bifurcation points. Around the super-critical bifurcation point, W becomes too large to load atoms enough to produce SSB in our experimental system. Near the sub-critical bifurcation point, on the other hand, despite the low N_c, only the population of the central stationary state among the triple wells increases, whereas those of the two dynamic states do not increase above N_c [11].

In order to have a better understanding of SSB, we have investigated the temporal evolution of the populations of each state when SSB occurs. Figure 2(b) shows the atomic populations recorded by the absorption of the probe laser. As can be found, in the initial loading stage, the number of atoms in each state increases at the same rate and their growth is indistinguishable with each other. As the loading process is finished at about 20 s elapse, however, the population of one state increases whereas the other state is depopulated. The fact that the total atomic number is conserved within experimental errors during the SSB process indicates that SSB originates not from different loading rates to each state but from the transfer of atoms from one state to the other. Moreover, when we place a kicking laser near the center of the two dynamic states in order to block any transitions between the states, the population symmetry is recovered. These evidences confirm that SSB occurs due to the atomic transfer between the two states.

Based on the fact that SSB appears above the critical number, one may conjecture that the underlying mechanism of SSB is related to the collective effects of atoms occurring between the two dynamic states [12,13,14,15]. There are two such collective mechanisms associated with the MOT atoms. One is the shadow effect caused by absorption of the cooling lasers in the z-axis due to atoms in one of the two states, which results in the reduction of the laser intensity for atoms in the other state. The other is the reradiation effect that arises when an atom reabsorbs photons that are spontaneously emitted by another atom, which produces the repulsive Coulomb-like forces between the two atoms.

The reradiation effect, in fact, contributes as an obstacle to SSB. As the number of atoms in one of the two states becomes dominated due to fluctuations, the repulsive reradiation force becomes bigger outside the more-populated atomic cloud. As a result, this effect prevents atoms in the smaller-number state from being transferred to the larger-number state, which results in the recovery of population symmetry between the two states. On the other hand, the shadow effect accelerates atoms to move from the smaller-number state to the larger-number state: due to the bigger shadow effects associated with the larger-number state, the net atomic force is directed toward the larger-number state, which enhances SSB further.

For a theoretical understanding of SSB process, we have adopted the phase-space Hamiltonian-function formalism developed in Ref. [18] to account for the transitions between the dynamic double wells [11]. We then have generalized the approach to include the shadow effect as well as the reradiation force. This approach provides quantitative analysis of nearly all the fundamental characteristics of SSB such as the critical number and the temporal evolution.

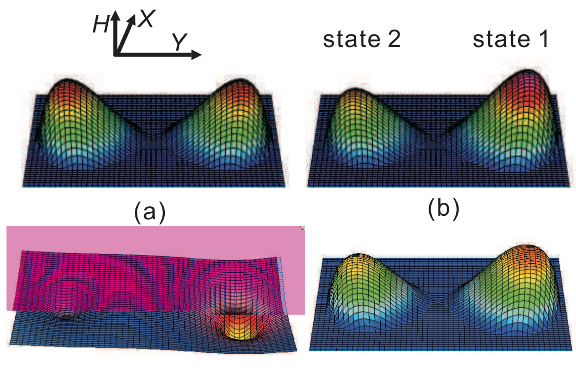

FIG. 3: (a) Hamiltonian function $H_i^0(X_i;Y_i)$ [Eq. (1)] for the symmetric state without collective effects. (b) $H_i^0 + H_i^S$ with the shadow effect included, which leads to SSB in the phase-space potential. (c) Reradiation interaction H_i^R, which opposes SSB. (d) $H_i^0 + H_i^S + H_i^R$, which shows slightly reduced SSB with respect to (b). Here $N_1 = 3 \quad 10^8$, $N_2 = 1 \quad 10^8$, $I_z = 0.035 I_s$, $I_T = 8 I_z$, $b = 14$ G/cm, $= 2.5$, $f = 2f_0$, $h = 0.9$, and the transverse (longitudinal) spatial width of the atomic cloud is $R = 1$ mm ($R_z = 2$ mm).

From the Doppler equation of MOT [11, 16], one can derive the phase-space Hamiltonian function of an i-th atom without the collective effects as,

$$H_i^0(X_i;Y_i) = \frac{1}{2}(\quad 1)X_i^2 + \frac{1}{2}(\; + 1)Y_i^2 \quad \frac{1}{4}(X_i^2 + Y_i^2)^2 ; \quad (1)$$

where $= 2(f \quad 2f_0)=hf_0$, X_i and Y_i are the two scaled canonical variables in the rotating phase space, as represented in Fig. 3(a). The total Hamiltonian H_0 without the interaction terms is just the summation of each H_i^0, $H_0 = \sum_{i=1}^{N_T} H_i^0$. Note that, in our analysis, the two oscillating atomic states can be approximated as a static double well in the phase space [Fig. 3(a)]. For example, the right- and left-side cloud with respect to the center of the limit cycle motion along the z-axis corresponds to the positive and negative state, respectively, in the Y axis at a given modulation phase of 0. Note also that the maximum points in the phase-space potential in Fig. 3 indicate attractors.

Let us first consider the shadow effect that is responsible for SSB. At the specific modulation phase of 0, we assume the right-side atomic cloud is the state 1 and the left-side cloud is the state 2. Because of the Zeeman shift, atoms in state 2 and state 1 absorb preferentially the cooling lasers propagating in the +z and z direction, respectively. Now we consider another j-th atom in state 1 or 2, which absorbs the laser by the amount $I_A^j = {}_L^j n \, I_z$, where ${}_L^j$ is the absorption cross-section of the j-th atom and n is the density of atoms in the xy-plane. One can then easily find that each laser photon absorbed by the j-th atom effectively results in a cooperative force (or acceleration) on the i-th atom concerned, whose magnitude is given by $C_S \; {}_L^j n \; I_z = I_s$. That is, when the atom j is in state 1 (i.e., in the right-side cloud absorbing the photons propagating in the -z axis), the direction of the effective force experienced by the i-th atom is positive along the z-axis, whereas it is negative when the j-th atom is in state 2. If one considers, for convenience, the i-th atom is near the center, the net effective force exerted on the i-th atom is given by $\sum_j C_S I_A^j = I_s = (N_1 \quad N_2) C_S I_A = I_s$. Therefore the i-th atom is transferred to the larger-number state on the right (state 1) [Fig. 3(b)]. Note that if one considers the phase of modulation, although the location of state 1 (2) is now exchanged to the left (right), the net force is still directed to the larger-number state of 1.

The Hamiltonian H_i^S for the shadow effect is then derived as, when summed over j in the states 1 and 2,

$$\begin{aligned} H_i^S(X_i;Y_i) &= \sum_{j2 1;2} (\; {}_j Y_i + H^0{}_j) ; \\ &= (N_1 \quad N_2) Y_i + (N_1 + N_2) H^0 ; \quad (2) \end{aligned}$$

where ${}_j = \; = 2C_S \; {}_L I_z = I_s \; {}^2 \; {}^{3=2} \; f2 \; R^2$ (${}_L^j$ is assumed independent of j), $C_S = hk = 2m(1 + 4 \; ^2 = \; ^2)$, $= 2 \; hf_0^2 = f$, $= \sqrt{4 \quad ff_0^2 = 3A_0(\; ^2 + 4 \; ^2 f_0^2)}$, is the damping coefficient, and A_0 is the coefficient of the third-order term in the Doppler equation of MOT [16]. H^0 is a given coefficient that is practically independent of j, with no contribution to SSB. Here ${}_L$ is regarded as having no dependence on velocity and position of atoms, which are assumed uniformly distributed in the xy-plane. We will discuss later about more realistic treatment of the shadow effect with Monte-Carlo simulations. As shown in Fig. 3(b), the shadow effect makes the potential of the larger-number state (state 1) deeper, whereas that of the smaller-number state (state 2) shallower. As a result, more atoms will be transferred from state 2 to state 1, resulting in SSB of the atomic population. In fact, however, there are competitions between the shadow-induced SSB and the fluctuation-induced symmetry-recovering transition. Therefore the critical number is determined by the balance between the shadow effect and the diffusion.

Let us now consider the symmetry-preserving reradiation effect. Figure 3(c) presents the results of reradiation interaction H_i^R, which reduces the SSB effect (detailed expression of H_i^R will be given elsewhere). Briefly speaking, the reradiation effect increases the critical number by reducing to C_R, where $C_R = I_T \; {}_L^2 = 4 \; c[3 \; + 8(4 + 3 \ln 2)] = 6 \; ^2 R_z \; ^2 \; ^2 f$. The calculation also shows that, if the transverse laser intensity is over 10 times larger than that of the z-direction laser, the reradiation effect dominates over the shadow effect, which inhibits SSB for every N_T. In practice, we have experimentally observed that the recovery of symmetry appears at about 20 times the z-laser intensity, which is a strong and independent evidence that the reradiation hinders SSB.

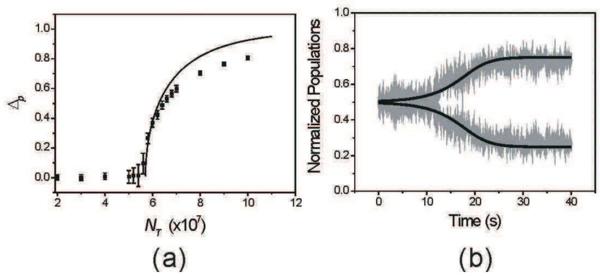

FIG. 4: (a) Δ_p vs N_T, obtained by Monte-Carlo simulations with 10^3 atoms. The solid curve is a plot of Eq. (3). (b) Simulation curves for the temporal evolution of SSB, in good agreement with the experimental data (Fig. 2(b)). Here $W_0 = 1.0\ s^{-1}$ and $N_T = 1.1N_c$.

Let us discuss the temporal evolution of SSB, which can be described by the simple rate equation, $d\Delta_p/dt = W_{12}(1+\Delta_p) + W_{21}(1-\Delta_p)$, where the transition rate $W_{12(21)}$ from state 1 (2) to state 2 (1) is $W_0 \exp(\mp\Delta_p N_T/N_c)$ and $N_c = D/2\sqrt{\ +1}f(\ )$. Here W_0 is the atomic transition rate without the collective effects, D is the phase-space diffusion constant [11], and $f(\ )$ is an $O(1)$ function [18]. Interestingly, the above rate equation leads to the steady-state solution given by

$$\Delta_p = \tanh(\Delta_p N_T/N_c): \tag{3}$$

This is a representative equation of Ising-class phase transition, which is plotted in Figs. 2(a) and 4(a).

To manifest further the relation with the Ising model, let us consider a simplified model where each atom i either belongs to state 1 ($Y_i = \sqrt{\ +1}$) or to state 2 ($Y_i = -\sqrt{\ +1}$). The activation energy S_i due to the shadow effect of the j-th atom is $2f(\ )\,{}_jY_i$. The total interaction energy is thus $\sum_i \sum_j^{N_T} S_i = -(J/2)(N_1 - N_2)^2$, where $J = 2f(\ )\sqrt{\ +1}$. The free energy of this model system is then $F = -(J/2)(N_T\Delta_p)^2 + DN_T\{[(1+\Delta_p)/2]\ln[(1+\Delta_p)/2] + [(1-\Delta_p)/2]\ln[(1-\Delta_p)/2]\}$. The equilibrium value of Δ_p is determined by the condition $\partial F/\partial\Delta_p = 0$, which results in $\Delta_p = \tanh(\Delta_p N_T J/D)$ that is exactly the same as Eq. (3) with $N_c = D/J$. The simple analytical values of N_c are in qualitative agreement with the experimental results of Fig. 2(a).

We also have performed Monte-Carlo simulations with more realistic consideration of the shadow effect and the reradiation force: we included the dependence of δ_L on the position and velocity, the transverse laser-intensity profile, and the random forces due to spontaneous emissions. Figure 4(a) shows Δ_p versus N_T, which is very similar to the experimental results in Fig. 2(a). Figure 4(b) presents the simulation curves for the temporal evolution of SSB. Here we have just included the shadow effect and used a diffusion constant that is 2.5 times the value derived from the simple Doppler theory. When the reradiation force is included in the simulations, however, N_c is slightly increased and SSB does not occur if the transverse laser intensity is over 10 times the z-laser intensity. In conclusion, nonlinear dynamic study of driven cold atoms may be useful for dynamic phase transition and temporal dependence of critical phenomena.

Acknowledgments

This work was supported by the CRI Project of the MOST of Korea. H.R.N. was supported by Korea Research Foundation Grant (KRF-2004-041-C00149).

[1] S. O. Demokritov, et. al., Nature (London), 426 159 (2003).
[2] F. S. Zhang and R. M. Lynden-Bell, Phys. Rev. Lett. 90 185505 (2003).
[3] C. Cambournac, et. al., Phys. Rev. Lett. 89 083901 (2002).
[4] J. Eggers, Phys. Rev. Lett. 83, 5322 (1999).
[5] J. Javier Brey, et. al., Phys. Rev. E 65, 011305 (2001).
[6] P. Hanggi, P. Talkner, and M. Borkovac, Rev. Mod. Phys. 62, 251 (1990).
[7] A. Simon and A. Libchaber, Phys. Rev. Lett. 68, 3375 (1992).
[8] L. I. McCann, M. I. Dykman, and B. Golding, Nature (London) 402, 785 (1999).
[9] D. B. Luchinsky, and P. V. E. McClintock, Nature (London) 389, 463 (1997).
[10] L. J. Lapidus, D. Enzer, and G. Gabrielse, Phys. Rev. Lett. 83, 899 (1999).
[11] K. Kim, et. al., to be published.
[12] J. Dalibard, Opt. Commun. 68, 203 (1988).
[13] T. Walker, et. al., Phys. Rev. Lett. 64, 408 (1990); D. G. Sesko, et. al., J. Opt. Soc. Am. B 8, 941 (1991).
[14] I. Guedes, et. al., J. Opt. Soc. Am. 11, 1935 (1994); V. S. Bagnato, et. al., Phys. Rev. A 48, 3771 (1993); D. Felinto, et. al., Phys. Rev. A 60, 2591 (1999).
[15] D. Wilkowski, et. al., Phys. Rev. Lett. 85, 1839 (2000).
[16] K. Kim, et. al., Phys. Rev. A 68, 031403(R) (2003); K. Kim, et. al., Opt. Comm. 236 349 (2004).
[17] K. Kim, H.-R. Noh, and W. Jhe, 71, 033413, (2005); K. Kim, K.-H. Lee, M. Heo, H.-R. Noh and W. Jhe, 71, 053406, (2005).
[18] M. I. Dykman, et. al., Phys. Rev. E 57, 5202 (1998).
[19] K. Huang, Statistical Mechanics (John Wiley, New York, 1987).